Optics Communications 402 (2017) 489–497

Contents lists available at ScienceDirect

Optics Communications

journal homepage: www.elsevier.com/locate/optcom

Phase extraction for dual-wavelength phase-shift Fizeau interferometry in the presence of multi-beam interference

Jinlong Cheng [a], Qun Yuan [a], Yimeng Dou [a], Yanxia Yao [a], Jialing Huang [a], Chao Zuo [a,b], Zhishan Gao [a,*]

[a] School of Electronic and Optical Engineering, Nanjing University of Science and Technology, Nanjing, 210094, China
[b] Nanjing University of Science and Technology, Jiangsu Key Laboratory of Spectral Imaging & Intelligence Sense, Xiaolingwei 200#, Nanjing, 210094, China

ARTICLE INFO

Keywords:
Interferometry
Phase measurement
Dual-wavelength
High reflection
Multi-beam interference
Phase-shift error

ABSTRACT

Dual-wavelength interferometry could extend the measured range of single-wavelength interferometry by combining the two single wavelength phases, particularly for the measurement of step height. When testing the high-reflectivity surfaces with the single wavelength Fizeau interferometer, we have presented the $\pi/4$ phase-shift carrier squeezing interferometry (QCSI) method for phase extraction with multi-beam interference (*Appl. Opt.* 55, 1920–1928, 2016). In this paper, we propose an integer and decimal portions synthetization (IDS) method for the multi-beam interference in the dual-wavelength Fizeau interferometer. One of the single wavelength wrapped phases is demodulated by the multi-beam interference QCSI algorithm, while the second of the single wavelength wrapped phases is extracted by the conventional two-beam interference phase-shift algorithm, so the equivalent wavelength unwrapped phase is derived from the two single wavelength wrapped phase. The decimal portion of synthesized phase is then obtained directly from the first single wavelength wrapped phase, and the integer portion of synthesized phase is obtained from the fringe order of the first single wavelength wrapped phase determined by the equivalent wavelength unwrapped phase. The proposed non-iterative IDS method avoids the common error magnification effect in the two-wavelength techniques, and only requires no more than 8 frame phase-shift interferograms for each single wavelength. Its robust performance is validated by both simulations and experiments in the presence of multi-beam interference as well as phase-shift error for measuring objects with height discontinuities.

1. Introduction

The interferometry is a powerful, typical and direct choice to measure the three-dimensional surface profile [1]. However, if the surface has a height discontinuity larger than a quarter of the wavelength of the illumination laser, the profile cannot be measured correctly using single-wavelength interferometry, due to the 2π phase ambiguity problem in the phase unwrapping procedure. Dual-wavelength interferometry provides a solution to solve this problem [2,3]. Subtracting the unwrapped phase at the first wavelength from the other unwrapped phase at the second wavelength, the phase for the long equivalent wavelength is produced, enabling measurement of height discontinuities larger than $\lambda/4$ at either single wavelength. A variety of remarkable researches to demodulate the phase for the equivalent wavelength have been reported, which are based on the two-beam interference [4–6].

However, when testing surface with high reflectivity, the multi-beam interference exists and the interference intensity is not strictly cosine distributed [7,8]. The ripple error presents obviously in the extracted phase for the equivalent wavelength from the combination of the two phases at each single wavelength when using the routine phase-shift algorithms suitable only for two-beam interference. Placing an attenuator in interferometric cavity is a usual approach to suppress multi-beam interference. However, for the test surfaces with different reflectivity or apertures, attenuators should be fabricated with different transmissivities or apertures at both of the two wavelengths in dual-wavelength Fizeau interferometry.

The other way to handle this problem is to separately demodulate the phase at each single wavelength using the multi-beam interference algorithms. These multi-beam interference algorithms have been made aiming at reducing the effect of harmonics, which could be divided into

* Corresponding author.

http://dx.doi.org/10.1016/j.optcom.2017.06.066
Received 17 February 2017; Received in revised form 16 June 2017; Accepted 19 June 2017
0030-4018/

the non-iterative and iterative methods according to the demodulation process. The multi-beam interference error could be suppressed by the $\pi/4$ phase-shift averaging method [9], principal component analysis (PCA) [10–12], 4N-3 algorithm [13,14] and so on, all of which are non-iterative algorithms. However, their precision is limited by the accuracy of phase shift. Using the iterative algorithm, phase distribution can be extracted from the interferograms with random phase shifts [15,16]. Actually, the phase shifts in the well-calibrated Fizeau interferometer are not arbitrary but with minor difference from the demanded nominal value, so the time-consuming iterative algorithm will not be the best choice. To suppress the ripple error in the retrieved phase induced by the multi-beam interference and the phase-shift errors simultaneously, a $\pi/4$ phase-shift carrier squeezing interferometry (QCSI) algorithm is proposed [17], which is based on carrier squeezing interferometry (CSI) by converting the temporal phase shift into spatial carrier and establishing the relationship of the temporal domain and spatial domain [18–20]. However, as mentioned above, the equivalent wavelength phase is obtained by subtracting the phase at one wavelength from the phase at the other wavelength. Therefore, both phases should be demodulated by the multi-beam interference algorithms mentioned above respectively, which would be a complex and time-consuming process. Moreover, for the error magnification effect in the two wavelength techniques [2], all the retrieve errors of the two single-wavelength phases would be superposed and magnified in the equivalent wavelength phase.

This paper is organized mainly as follows. In Section 2, for single wavelength phase in the presence of multi-beam interference as well as phase-shift error, the calculated residual phase error by the conventional phase-shift algorithm such as the de Groot 7-frame algorithm [21] is analyzed. Based on the analysis of the demodulated phase error and the two-wavelength techniques, we present an integer and decimal portions synthetization (IDS) method for multi-beam interference in the dual-wavelength Fizeau interferometer in Section 3. By the calculation of the integer-portion phase, the residual phase error for the conventional phase-shift algorithm could be suppressed. And then one of the single-wavelength wrapped phases could be extracted by the multi-beam interference algorithm, while the second could be demodulated by the conventional two-beam interference phase-shift algorithm. So the process of phase demodulation is simplified by the proposed IDS method. Finally, in Sections 4 and 5, numerical simulations and experiments are executed to demonstrate the performance of the proposed IDS method in multi-beam interference, compared with the 7-frame algorithm, $\pi/4$ phase averaging algorithm and the iterative algorithm.

2. Analysis for the demodulated error

In the presence of multiple-beam interference as well as phase-shift error for Fizeau interferometer, the calculated residual phase error for the conventional phase-shift algorithm could be expressed as:

$$\Delta\phi = o\left(a_i\right) + o\left(\varepsilon_j\right) \tag{1}$$

where $o\left(a_i\right)$ and $o\left(\varepsilon_i\right)$ are the residual calculated phase errors resulted by the harmonics in multi-beam interferometry and the phase-shift error separately, and a_i is the coefficients of harmonic in multi-beam interferometry, while ε_i is the error coefficient of phase shift. To estimate the influences of the retrieve errors for the single-wavelength phase in dual-wavelength interferometry, the multi-beam interferometry error $o\left(a_i\right)$ and phase-shift error $o\left(\varepsilon_i\right)$ would be analyzed separately in following section.

2.1. demodulated error in presence of multi-beam interference

The intensity distribution of multi-beam interference in Fizeau interferometer could be developed in Fourier series from the expression of the Airy formula [22]. And the intensity distribution of multi-beam interference could be expressed approximately as the sum of harmonics [23]:

$$I_n = I_0\left\{\frac{a_0}{2} + \sum_{k=1}^{\infty} a_k \cos\left[k\cdot\left(\phi+\delta_n\right)\right]\right\} \tag{2}$$

where I_0 and ϕ are the local mean intensity and measured phase separately, and δ_n is the temporal phase shift, and n is the frame number, and the pixel coordinate (x, y) in Eq. (2) is omitted for simplicity. Besides, the coefficients in Eq. (2) are depended on the reflection coefficients of reference flat r_1 and test surface r_2, which are defined as follows:

$$a_0 = \frac{2\left(r_1^2 + r_2^2 - 2r_1^2r_2^2\right)}{1 - r_1^2r_2^2} \tag{3}$$

$$a_k = \frac{2\left(1-r_1^2\right)\left(1-r_2^2\right)}{r_1^2r_2^2 - 1}\left(r_1r_2\right)^k, \quad k = 1, 2, \ldots. \tag{4}$$

For the conventional phase-shift algorithm such as the 7-frame phase-shift algorithm proposed by de Groot [21], the calculated phase error $o\left(a_i\right)$ in Eq. (1) from the multi-beam interferograms with $\pi/2$ phase shift could be expressed as:

$$o\left(a_i\right) = \sum_{m=1}^{\infty}\left[\frac{\left(a_{(4m-1)} - a_{(4m+1)}\right)}{a_1}\sin\left(4m\phi\right) - \frac{1}{2}\frac{\left(a_{(4m-1)} - a_{(4m+1)}\right)}{a_1}\frac{\left(a_{(4m-1)} + a_{(4m+1)}\right)}{a_1}\sin\left(8m\phi\right) + \cdots\right]. \tag{5}$$

The term of $\sin\left(8m\phi\right)$ and the higher order ones in Eq. (5) could be omitted due to their small coefficients. The calculated error is then approximated as the sinusoidal function with the period 4 times the modulation frequency of fringes. And substituting the coefficients of harmonics in Eqs. (3) and (4) into Eq. (5), the calculated phase error $o\left(a_i\right)$ could also be rewritten as:

$$o\left(a_i\right) = r_1^2r_2^2\left(1 - r_1^2r_2^2\right)\cos\left(4\phi\right). \tag{6}$$

Since the reflection coefficients $r_1, r_2 < 1$, the coefficient of sine term in Eq. (6) satisfies the condition:

$$r_1^2r_2^2\left(1 - r_1^2r_2^2\right) < \frac{1}{2}\left[r_1^2r_2^2 + \left(1 - r_1^2r_2^2\right)\right]^2 = \frac{1}{2}. \tag{7}$$

Therefore the calculated phase error of 7-frame phase-shift algorithm for multi-beam interferometry satisfies the condition $o\left(a_i\right) < 1/2$ rad. To provide a more intuitive explanation, Fig. 1 illustrates the values of the coefficient for sine term in the calculated phase error $o\left(a_i\right)$ in Eq. (6) with the test surface reflection coefficient r_2 varying from 0.2 to 0.99, while the reflection coefficient of reference flat r_1 is set from 0.2 to 0.9. Inferred from the relationship curve presented in Fig. 1, the value of the coefficient in Eq. (6) is less than 0.3. And then the values of calculated phase error satisfies the condition $o\left(a_i\right) < 0.3$ rad.

Actually in dual-wavelength Fizeau interferometer developed by ourselves with the working wavelength 632.8 nm and 532 nm, the reference flat is made by silica with the reflection coefficient about 0.2. Therefore, the values of calculated phase error satisfies the condition $o\left(a_i\right) < 0.04$ rad from Fig. 1.

2.2. demodulated error in presence of phase-shift error

When the phase shifter is not calibrated well and is non-linear for the existence of the phase-shift error, the phase shift δ_n could be expressed as a function of the unperturbed phase-shift values δ_{0n}, which is given by the superposition of different-order polynomials:

$$\delta_n = \delta_{0n}\left[1 + \varepsilon_1 + \varepsilon_2\frac{\delta_{0n}}{\pi} + \varepsilon_3\left(\frac{\delta_{0n}}{\pi}\right)^2 + \cdots + \varepsilon_p\left(\frac{\delta_{0n}}{\pi}\right)^{p-1}\right], \quad n = 1, \ldots, N \tag{8}$$

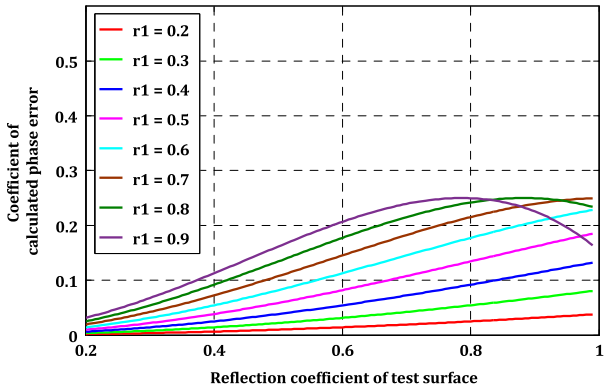

Fig. 1. The values of the coefficient for sinusoidal term in $o(a_i)$ with r_2 varying from 0.2 to 0.99, while r_1 is set from 0.2 to 0.9.

where p $(p < N-1)$ is the maximum order of the nonlinearity, and ε_q $(1 \le q \le p)$ is the qth order error coefficient, which is smaller than 1. Staying with de Groot's 7-frame phase-shift algorithm, the calculated residual phase error $o(\varepsilon_j)$ in Eq. (1) caused by the phase-shift error could be expressed as [24]:

$$o(\varepsilon_j) = \frac{\pi}{2}\varepsilon_2 - \frac{\pi^2\varepsilon_2^2}{64}\sin(2\phi) + \frac{\pi^4\varepsilon_1^4}{256}\sin(2\phi) + \cdots \tag{9}$$

where the phase shift δ_n is given by the superposition of the first two order polynomials for simplicity:

$$\delta_n = \frac{\pi}{2}(n-3)\left[1 + \varepsilon_1 + \frac{\varepsilon_2}{2}(n-3)\right], \quad n = 1, 2 \ldots N. \tag{10}$$

From the calculated residual phase error $o(\varepsilon_j)$ in Eq. (9), the dc component $\pi\varepsilon_2/2$ is a constant for a spatially uniform phase shift, which would not affect the extraction of the measured phase. For the error coefficient ε_q is smaller than 1, the higher order residual error could be neglected. And the calculated residual phase error $o(\varepsilon_j)$ in Eq. (9) caused by the phase-shift error could be rewritten and satisfies the condition:

$$\begin{aligned} o(\varepsilon_j) &\approx -\frac{\pi^2\varepsilon_2^2}{64}\sin(2\phi) + \frac{\pi^4\varepsilon_1^4}{256}\sin(2\phi) \\ &\le \left|-\frac{\pi^2\varepsilon_2^2}{64} + \frac{\pi^4\varepsilon_1^4}{256}\right| = \frac{\pi^2}{64}\cdot\left|-\varepsilon_2^2 + \frac{\pi^2\varepsilon_1^4}{64}\right| < \frac{\pi^2}{64} \end{aligned} \tag{11}$$

Therefore the calculated phase error $o(\varepsilon_j)$ in Eq. (9) satisfies the condition $o(\varepsilon_j) < \pi^2/64 = 0.16$ rad. And Fig. 2 illustrates the maximum value of calculated residual phase error $o(\varepsilon_j)$ caused by the phase-shift error for de Groot's 7-frame phase-shift algorithm. The 2nd order error coefficient ε_2 is set from −0.3 to 0.3 with the phase-shift miscalibration varying from −0.3 to 0.3, which is sufficient to present the most cases for the phase-shift errors. Derived from Fig. 2, the values of calculated phase error $o(\varepsilon_j)$ caused by the phase-shift error for de Groot's 7-frame phase-shift algorithm satisfies the condition $o(\varepsilon_j) < 0.02$ rad actually.

As analyzed above, the varying ranges for the residual calculated phase errors resulted by the harmonics in multi-beam interferometry and the phase-shift error are $o(a_i) < 1/2$ rad and $o(\varepsilon_j) < 0.16$ rad separately. And then the calculated residual phase error in Eq. (1) resulted by the harmonics in multi-beam interferometry and the phase-shift error for the conventional phase-shift algorithm satisfies the condition:

$$\Delta\phi = o(a_i) + o(\varepsilon_j) < 0.5 + 0.16 = 0.66\ rad. \tag{12}$$

Moreover, from the practical analysis of the residual calculated phase errors resulted by the harmonics in multi-beam interferometry and the phase-shift error shown in Figs. 1 and 2, we find that $o(a_i) < 0.04$ rad and $o(\varepsilon_j) < 0.02$ rad. Then the calculated residual phase error in Eq. (12) $\Delta\phi$ is less than 0.06 rad actually.

3. Principle of the proposed IDS method

In the two-wavelength techniques, the equivalent wavelength wrapped phase is obtained by subtracting the measured phases at two different wavelengths, which could be expressed as [2]:

$$\phi_{eq} = \phi_{\lambda_2} - \phi_{\lambda_1} = 2\pi\left(\frac{1}{\lambda_2} - \frac{1}{\lambda_1}\right)z = \frac{2\pi}{\lambda_{eq}}z \tag{13}$$

where λ_1 and λ_2 are the two wavelengths used to make the measurement, and λ_2 is assumed to be less than λ_1. ϕ_{λ_1} and ϕ_{λ_2} are the single-wavelength wrapped phases for λ_1 and λ_2 respectively, and $\lambda_{eq} = \lambda_1\lambda_2/(\lambda_1 - \lambda_2)$ represents the longer equivalent wavelength. And z is measured difference in surface height.

And from the equivalent wavelength phase in Eq. (13), the measured difference in surface height could be written as:

$$z = \frac{\phi_{eq}}{2\pi}\lambda_{eq} = \frac{\left(\phi_{\lambda_2} - \phi_{\lambda_1}\right)}{2\pi}\lambda_{eq} = \frac{\left(\phi_{\lambda_2} - \phi_{\lambda_1}\right)}{2\pi}M\frac{(\lambda_1 + \lambda_2)}{2} \tag{14}$$

where M is the wavelength magnification ratio and is defined as the ratio of long equivalent beat wavelength over the mean wavelength for λ_1 and λ_2. From Eq. (14), it is clear that the retrieval errors of the two single-wavelength phases would be superposed and amplified by the factor of M , adding to the true equivalent wavelength data. To improve the precision of the data, the equivalent wavelength unwrapped phase could be used to determine fringe orders of the single-wavelength data to remove the ambiguities [25].

Therefore, if the calculated phase error in Eq. (1) for the single wavelength could be suppressed in the determination of fringe orders for the other single wavelength, there is no need to use the multi-beam interferometry algorithm for the former in dual-wavelength phase-shift Fizeau interferometry with multi-beam interference. And the process would also be simplified. In addition, the precision of the measured data could be improved when the other one of single-wavelength phase is extracted by the multi-beam interference algorithm.

Specifically, the schematic of the procedure for the proposed IDS method is illustrated in Fig. 3. In IDS method, the multi-beam interferograms of the two single working wavelengths (such as λ_1 and λ_2) are processed by the multi-beam interferometry algorithm and the conventional phase-shift algorithm respectively, where the algorithms are the QCSI and 7-frame phase-shift algorithm separately. And then after the subtraction and unwrapping process, the practical unwrapped equivalent wavelength phase $\boldsymbol{\Phi}'_{\lambda_{eq}}$ could be obtained as:

$$\boldsymbol{\Phi}'_{\lambda_{eq}} = \boldsymbol{\Phi}_{\lambda_{eq}} + \Delta\phi_{\lambda_2} \tag{15}$$

where $\boldsymbol{\Phi}_{\lambda_{eq}}$ is the theoretical phase for λ_{eq}, and $\Delta\phi_{\lambda_2}$ is the residual calculated phase error of λ^2 demodulated by the conventional phase-shift algorithm in the presence of multi-beam interference, which is introduced in the equivalent wavelength phase by the subtraction.

As shown Fig. 3, the wrapped phase ϕ_{λ_1} of λ_1 demodulated by the multi-beam interferometry algorithm is used to be the decimal portions of final synthesized phase ϕ_{Dec}. And the equivalent wavelength phase $\boldsymbol{\Phi}'_{\lambda_{eq}}$ in Eq. (15) is used to calculate the fringe order of the single-wavelength λ_1 data and obtain the integer portions of final synthesized phase. Therefore, final synthesized phase could be written as:

$$\boldsymbol{\Phi} = \boldsymbol{\Phi}_{Int} + \phi_{Dec} = \boldsymbol{\Phi}_{Int} + \phi_{\lambda_1} \tag{16}$$

where $\boldsymbol{\Phi}_{Int}$ is the integer portion of final synthetized phase, and it could be expressed as:

$$\boldsymbol{\Phi}_{Int} = round\left[\frac{\boldsymbol{\Phi}'_{\lambda_{eq}}}{2\pi}\cdot\frac{\lambda_{eq}}{\lambda_1} - \frac{\phi_{\lambda_1}}{2\pi}\right]\cdot 2\pi \tag{17}$$

where round [ ] is the rounding operator. As mentioned above, when the unwrapped equivalent wavelength phase $\boldsymbol{\Phi}'_{\lambda_{eq}}$ with the calculated

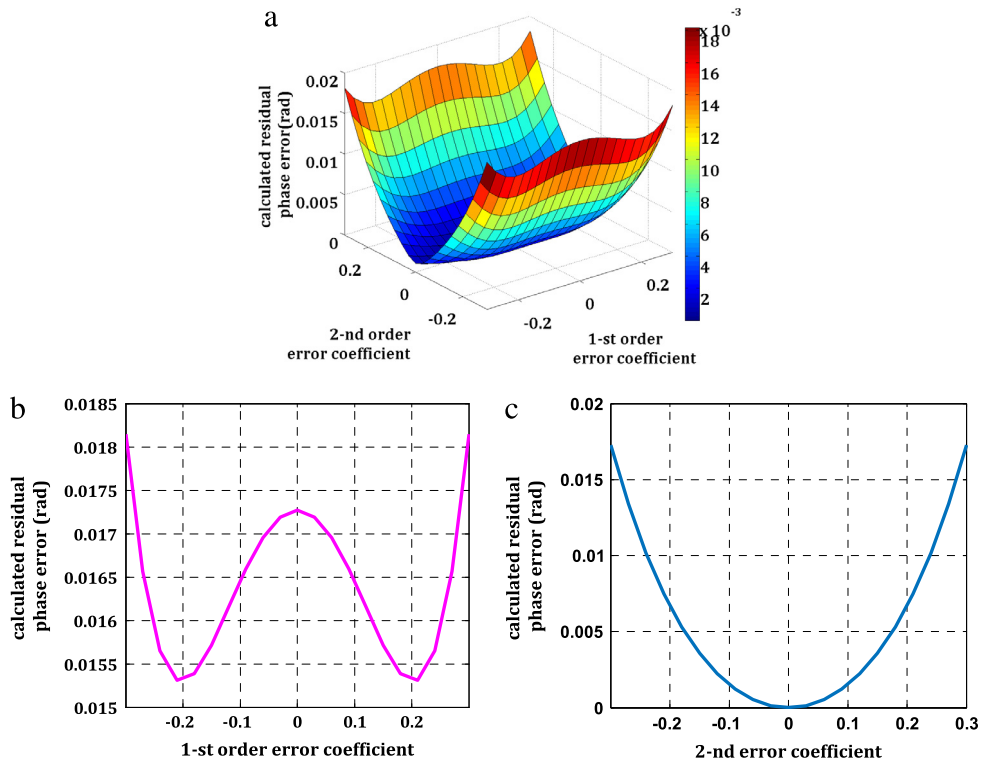

Fig. 2. The maximum values of calculated residual phase error $o(\varepsilon_j)$ caused by the phase-shift error for different the error coefficient ε_q using de Groot's 7-frame phase-shift algorithm: (a) ε_2 is set from −0.3 to 0.3 with the phase-shift miscalibration ε_1 varying from −0.3 to 0.3, (b) the phase-shift miscalibration ε_1 varied from −0.3 to 0.3 when ε_2 is set as 0.3, (c) ε_2 varied from −0.3 to 0.3 when ε_1 is set as 0.

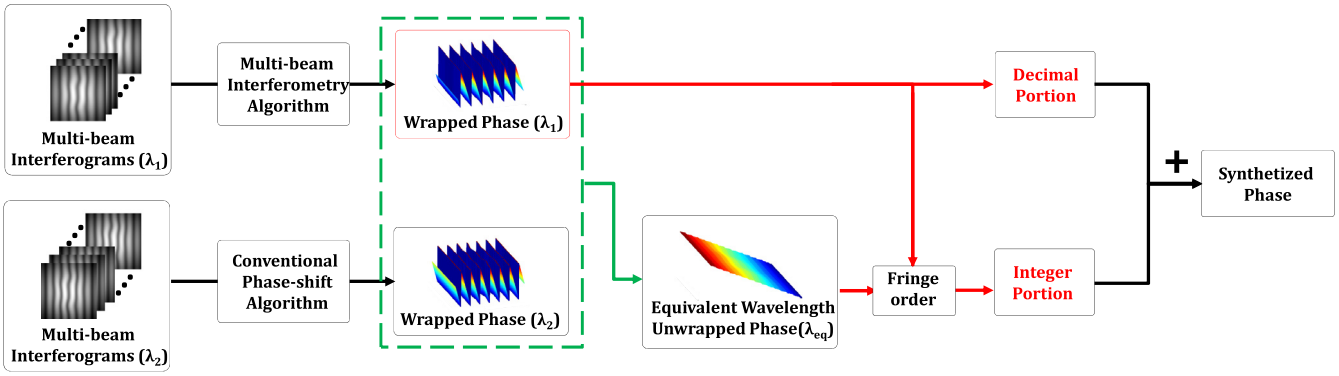

Fig. 3. The schematic of the procedure for the proposed IDS method.

residual error in Eq. (15) is substituted into Eq. (17) and the integer portion could be rewritten as:

$$\begin{aligned} \Phi_{Int} &= round\left[\frac{\Phi_{\lambda_{eq}}+\Delta\phi_{\lambda_2}}{2\pi}\cdot\frac{\lambda_{eq}}{\lambda_1}-\frac{\phi_{\lambda_1}}{2\pi}\right]\cdot 2\pi \\ &= round\left[\frac{\Phi_{\lambda_{eq}}}{2\pi}\cdot\frac{\lambda_{eq}}{\lambda_1}-\frac{\phi_{\lambda_1}}{2\pi}+\frac{\Delta\phi_{\lambda_2}}{2\pi}\cdot\frac{\lambda_{eq}}{\lambda_1}\right]\cdot 2\pi. \end{aligned} \tag{18}$$

Substituting the equivalent wavelength $\lambda_{eq} = \lambda_1\lambda_2/(\lambda_1-\lambda_2)$ into Eq. (18), the deviation of the integer portion phase introduced by the calculated phase error of λ^2 as the second term of round [ ] in the Eq. (18) could be derived as:

$$\Delta\Phi_{Int} = \frac{\lambda_2}{2\pi(\lambda_1-\lambda_2)}\Delta\phi_{\lambda_2}. \tag{19}$$

As shown in Eq. (18), when the deviation of the integer-portion phase $\Delta\Phi_{Int}$ in Eq. (19) is less than 1, it could be eliminated by the round operation in the calculation of the integer-portion phase as shown in Eq. (18). Therefore, the calculated phase error of λ_2 demodulated by the conventional phase-shift algorithm would not affect the final synthesized phase. In IDS method, the influence of multiple-beam interference error and phase-shift error for λ_1 could be suppressed using multi-beam algorithms, while the influence of calculated residual errors for λ_2 could be suppressed according to Eq. (18) with the round operation for the integer-portion phase.

And to obtain the varying range of the deviation of the integer-portion phase $\Delta\Phi_{Int}$ in Eq. (19), the residual calculated phase errors resulted by the harmonics in multi-beam interferometry and the phase-shift error by the conventional phase-shift algorithm have been analyzed in Section 2. As analyzed in Section 2 above, the varying range for the residual calculated phase error resulted by the harmonics in multi-beam interferometry and the phase-shift error is less than 0.66 rad as shown in Eq. (12). And then the deviation of the integer-portion phase in Eq. (19) could be derived theoretically as:

$$\Delta\Phi_{Int} < 0.105\frac{\lambda_2}{(\lambda_1-\lambda_2)}. \tag{20}$$

And as mentioned above, the deviation of the integer-portion phase $\Delta\Phi_{Int}$ could be eliminated by the round operation when it is less than 1. Therefore, the condition in Eq. (20) should be $0.105\lambda_2/(\lambda_1-\lambda_2) < 1$, and then the working wavelengths of the dual-wavelength Fizeau interferometer should satisfy the condition $\lambda_2 < 0.9\lambda_1$. Moreover, from the practical analysis of the residual calculated phase errors resulted by the harmonics in multi-beam interferometry and the phase-shift error shown in Figs. 1 and 2, the deviation $\Delta\Phi_{Int}$ is less than $0.06\lambda_2/(\lambda_1-\lambda_2)$. Therefore, the influence of calculated residual errors for λ_2 could be suppressed by IDS method when the working wavelengths satisfy the condition $\lambda_2 < 0.943\lambda_1$. And then the influence of the phase-shift errors and multi-beam interference for the single wavelength λ_2 in dual-wavelength Fizeau interferometer could be suppressed by the IDS method.

4. Numerical simulation and analysis

In this section, numerical simulations are executed for evaluating the performance of the proposed IDS method. Fig. 4(a) shows the simulated wavefront distribution with the resolution of 256 ×256 pixels. The primary simulated is defined by the peaks function $w = 0.015 \times 632.8 \times$ peaks (256) with a step height of 1200 nm. And the profile of the step is plotted in Fig. 4(b).

The intensity distribution of interferogram without noise is determined by the Eq. (2), where the local mean intensity is set as $I_0(x,y) = \exp\left[-\left(x^2+y^2\right)/20\right]$ in general. And the two wavelengths are set as 632.8 nm and 532 nm respectively, which satisfied the condition $\lambda_2 < 0.943\lambda_1$. And therefore the equivalent wavelength is 3.34 μm. The reflection coefficients of reference surface and test surface are set as 0.2 and 0.7 respectively. A linear carrier along the horizontal direction for simplicity is introduced, and the interferograms of the two wavelengths are shown in Fig. 4(c) and (d) respectively.

For comparison, the 7-frame algorithm [21], $\pi/4$ phase averaging algorithm [9] and the iterative algorithm [15] are adopted to process the two single-wavelength multiple-beam interferograms separately in the simulation. For IDS method as shown in Fig. 3, the influence of multiple-beam interference and phase-shift error for the single working wavelength λ_1 are suppressed by the multi-beam interferometry algorithm, while the calculated residual errors for the other single working wavelength λ_2 are suppressed by the round operation for the integral-portion phase. The precision of IDS method is mainly depended on the multi-beam interferometry algorithm for the single working wavelength λ_1. Therefore, the QCSI algorithm [17] is used as the multiple-beam interferometry algorithm for λ_1 in IDS method as shown in Fig. 3 for it is not limited by the accuracy of phase shift and without the iterative process. And the 7-frame algorithm is used to progress the multiple-beam interferograms of λ_2 in IDS method

First, for the phase-shift multi-beam interferograms without phase-shift errors, Fig. 5 shows the demodulated residual errors processed by the three algorithms mentioned above and the proposed IDS method. And the profiles of the middle row in the demodulated residual errors are also plotted in Fig. 5 for further details. The calculated results of the $\pi/4$ phase averaging algorithm, the iterative algorithm and the IDS method are better than the 7-frame algorithm, which also validate the equivalentness of the IDS in the presence of multi-beam interference. And the precision of IDS method is better than PV 0.005λ and RMS 0.0012λ ($\lambda = 632.8$ nm).

As for the 7-frame phase-shift algorithm, the calculated phase error for the single wavelength could be approximated as the function of $\sin(4\phi)$ from Eq. (6) after the higher order ones are omitted due to their small coefficients. Therefore, the calculated phase error for the equivalent wavelength could be written as:

$$\begin{aligned}\Delta\phi_{\lambda_s} &= K_{\lambda_2}\sin\left(4\phi_{\lambda_2}\right) - K_{\lambda_1}\sin\left(4\phi_{\lambda_1}\right)\\ &= \left(K_{\lambda_2}+K_{\lambda_1}\right)\sin\left(2\phi_{\lambda_{eq}}\right)\cos\left(2\phi_{\lambda_a}\right)\end{aligned} \tag{21}$$

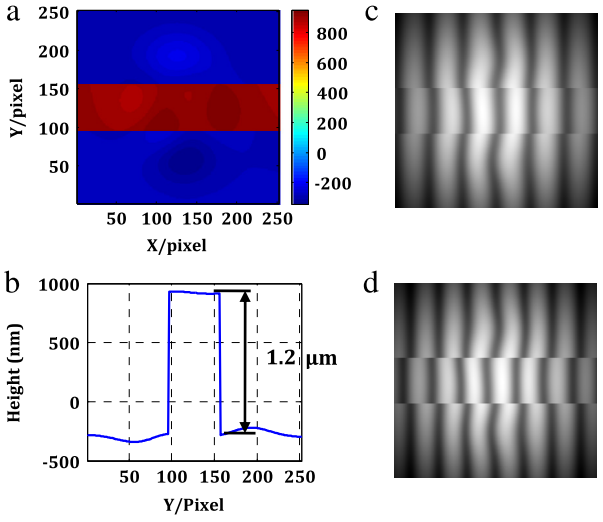

Fig. 4. Simulation results: (a) the given measured wavefront with a step of 1200 nm, (b) the profile of the step, (c) one of multiple-beam interferograms for 632.8 nm, (d) one of multiple-beam interferograms for 532 nm.

where K_{λ_1} and K_{λ_2} are the coefficients of the term $\sin(4m\phi)$ for the two working wavelengths separately. And $\phi_{\lambda_a} = \phi_{\lambda_1} + \phi_{\lambda_2}$ denotes the phase of the shorter averaging wavelength λ_a, which is represented by $\lambda_a = \lambda_1\lambda_2/(\lambda_1+\lambda_2) = 289$ nm. From Eq. (21), the calculated phase error for the 7-frame phase-shift algorithm is in the form of moiré fringe. And the modulation of the moiré is a sinusoidal function with the period 2 times frequency of the equivalent wavelength fringes. From the interferogram of the wavelength 632.8 nm as shown in Fig. 4(c), the equivalent wavelength interferogram is about 1.14 fringes. Considering about the 2 times characteristic of the modulation in the moiré, the modulation of the moiré ripple elements in the calculated phase is about $1.14\times2\times2 \approx 4.5$ fringes, which is in agreement with the result in Fig. 5(a). Similarly, after the term $\sin(4m\phi)$ form in the calculated phase error is suppressed by the $\pi/4$ phase averaging algorithm and the iterative algorithm, the calculated phase error for the equivalent wavelength phase could be approximated as $\Delta\phi_{\lambda_{eq}} = \left(K'_{\lambda_1}+K'_{\lambda_2}\right)\sin\left(4\phi_{\lambda_{eq}}\right)\cos\left(4\phi_{\lambda_a}\right)$, where K'_{λ_1} and K'_{λ_2} are the coefficients of the term $\sin(8m\phi)$ for the two working wavelengths separately. And then the modulation of the moiré ripple elements in the calculated phase error is about $1.14\times2\times4 \approx 9$ fringes, which could also be verified from the profile of the calculated phase error in Fig. 5(b) and (c).

Besides, the simulations are also executed with the phase-shift error, and the demodulated errors for the mentioned four algorithms above are illuminated in Fig. 6. In the simulation, the phase-shift error is determined by the 2-order polynomials in Eq. (8) with the order error coefficients $\varepsilon_1 = 0.2$ and $\varepsilon_2 = 0.2$, which is sufficient to the most practical cases for the phase-shift errors. As shown in Fig. 6, the precision of IDS method is better than the other three algorithms with the PV value of 5.42 nm (0.0086λ, $\lambda = 632.8$ nm) and RMS value of 1.13 nm (0.0018λ). For the deviation of $\pi/4$ phase shift between adjacent calculated phases in presence of the phase-shift error, the $\pi/4$ phase averaging algorithm could not suppress the influence of the multi-beam interference and the phase-shift error very well. And the iterative algorithm needs more multi-beam interferograms and iterations to improve the precision. Besides, all the retrieve errors of the two single-wavelength phases would be superposed and magnified in the equivalent wavelength phase for the error magnification effect, which could be avoided in IDS method.

Therefore, the precision of the proposed IDS method is better than the other algorithm for its superiority in suppressing the ripple error from the multi-beam interference as well as phase-shift error in dual-wavelength Fizeau interferometer.

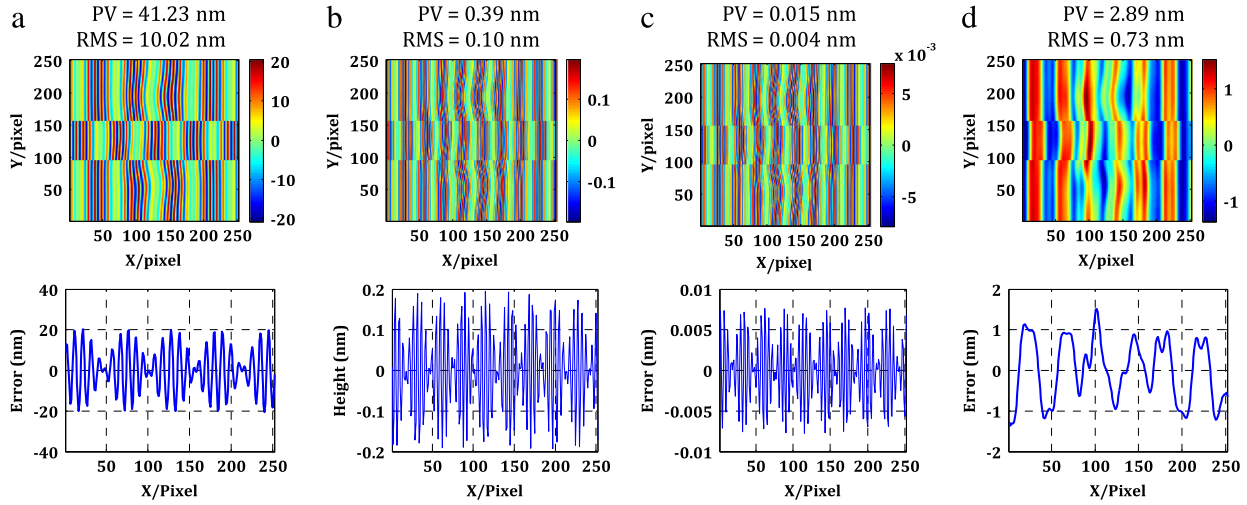

Fig. 5. Residual errors and the profiles of the middle row without the phase-shift error for 7-frame algorithm in (a), $\pi/4$ phase averaging algorithm in (b), the iterative algorithm in (c), and IDS method in (d).

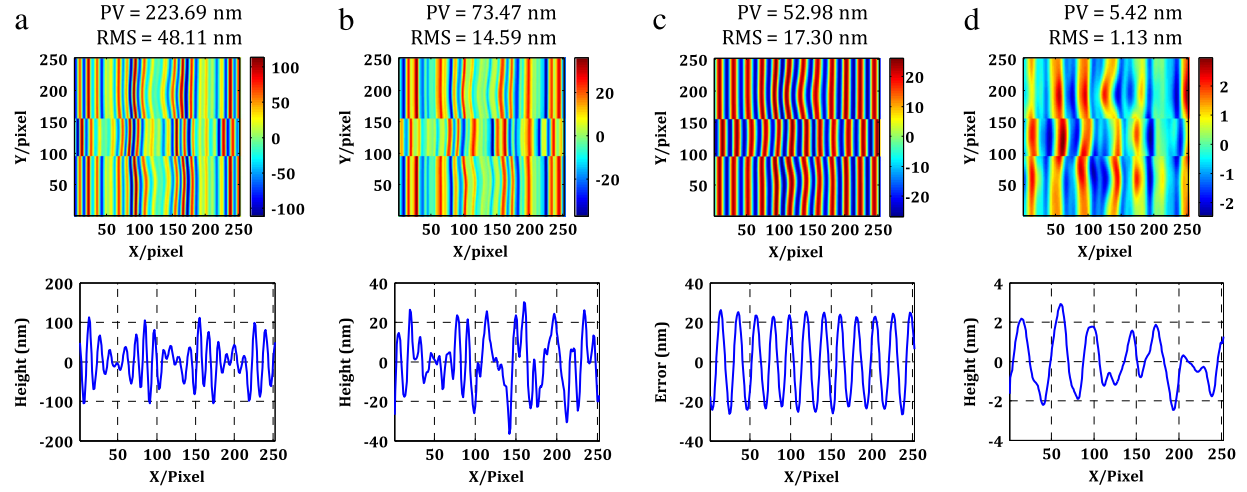

Fig. 6. Residual errors and the profiles of the middle row with the phase-shift error for 7-frame algorithm in (a), $\pi/4$ phase averaging algorithm in (b), the iterative algorithm in (c), and IDS method in (d).

5. Experiments

For a further comparison, the four algorithms above are applied in the experimental research to verify the performance of the proposed IDS method. The experiments are implemented in a dual-wavelength Fizeau interferometer developed by ourselves, with working wavelengths of 632.8 and 532 nm. And then the corresponding equivalent wavelength is equal to $\lambda_{eq} = 3.34$ μm. In addition the test sample with high reflectivity coefficient in the experiment is the veeco calibrated step with the height of 7.8 μm.

First, after the phase shifter is well calibrated, we capture the multiple-beam interferograms with $\pi/4$ phase shift for the two working wavelengths. And as mentioned above, the 7-frame algorithm, the $\pi/4$ phase averaging algorithm, the iterative algorithm and our proposed IDS method are used to these multi-beam interferograms for comparison. The final demodulated phases and the profiles of step for the above four algorithms are illustrated in Fig. 7. And the height results of the step for the four algorithms are also labeled in the figure.

To provide a more intuitive explanation and comparison, the distributions of the top and bottom surfaces for the test step demodulated by the four algorithms are illustrated in Fig. 8. As shown in the figure, the ripple presents in the retrieved phase demodulated by the 7-frame algorithm in Fig. 8(a), while disappears when using the other three algorithms. Besides, the distribution of the retrieved surface for the proposed IDS algorithm is in agreement with the results for the other two multi-beam interferometry algorithms, which validates the effectiveness of the IDS method in the presences of multi-beam interference. Meanwhile, the PV and RMS values of the top and bottom surfaces by the IDS algorithm are 516.72 nm (PV), 41.33 nm (RMS), 303.26 nm (PV) and 51.68 nm (RMS) respectively, which are better than the other two algorithms for the error magnification effect in the two-wavelength techniques.

Secondly, we also capture the phase-shift multiple-beam interferograms for the two wavelengths without calibrating the phase shifter. The same process as above is also implemented, and the final demodulated phases and the profiles are illustrated in Fig. 9 for comparison. In addition, the phase-shift error of experimental interferograms for the two working wavelengths is calculated by the iterative algorithm, which is shown in Fig. 10. And the maximal absolute value of the phase-shift error for the working wavelength 532 nm is 0.1338π, which is 53% relative to $\pi/4$.

For the existence of the phase-shift errors and the multi-beam interference, the ripple error presents in the retrieved phase demodulated by the 7-frame algorithm shown in Fig. 9(a) and the $\pi/4$ phase averaging algorithm shown in Fig. 9(b). For the deviation of $\pi/4$ phase shift between adjacent calculated phases, the $\pi/4$ phase averaging algorithm could not suppress the multi-beam interference error very well. And the ripple error disappears when using the iterative algorithm and our

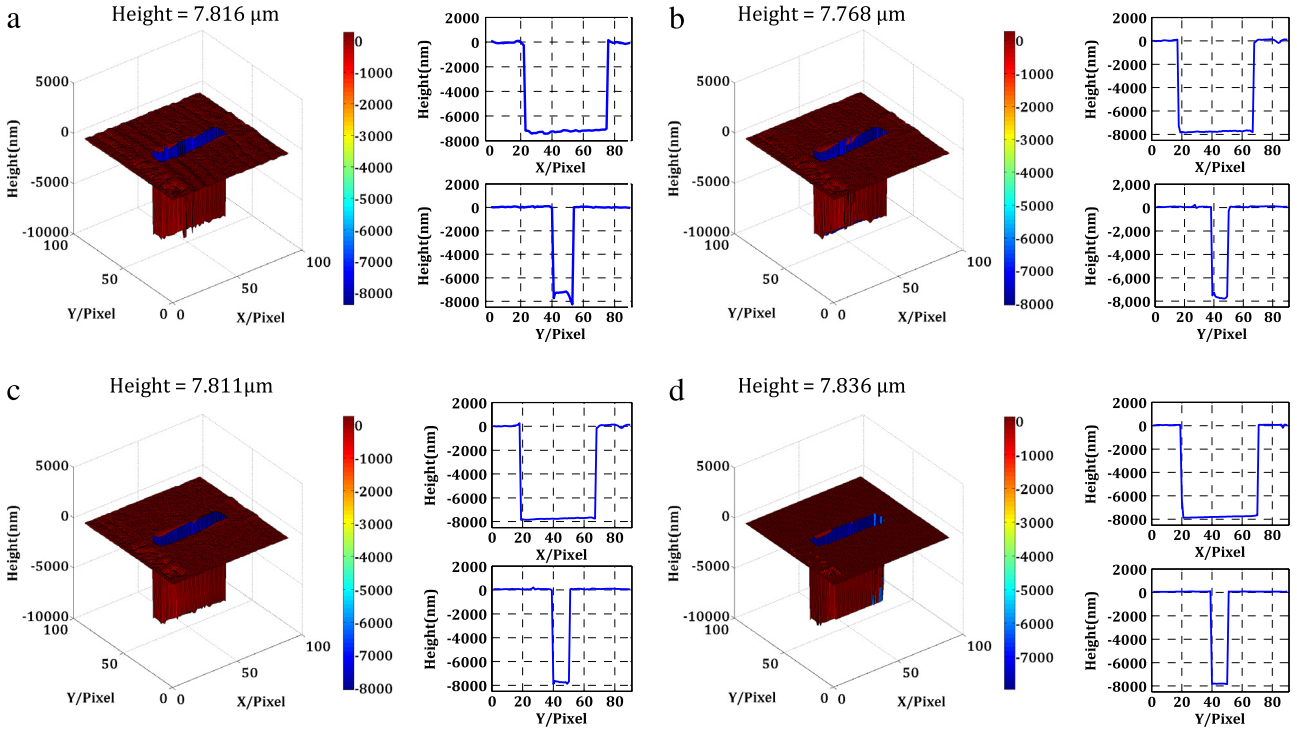

Fig. 7. Experimental results with the well calibrated phase shifter: the demodulated phases and profiles of the step by 7-frame algorithm in (a), $\pi/4$ phase averaging algorithm in (b), the iterative algorithm in (c), and IDS method in (d).

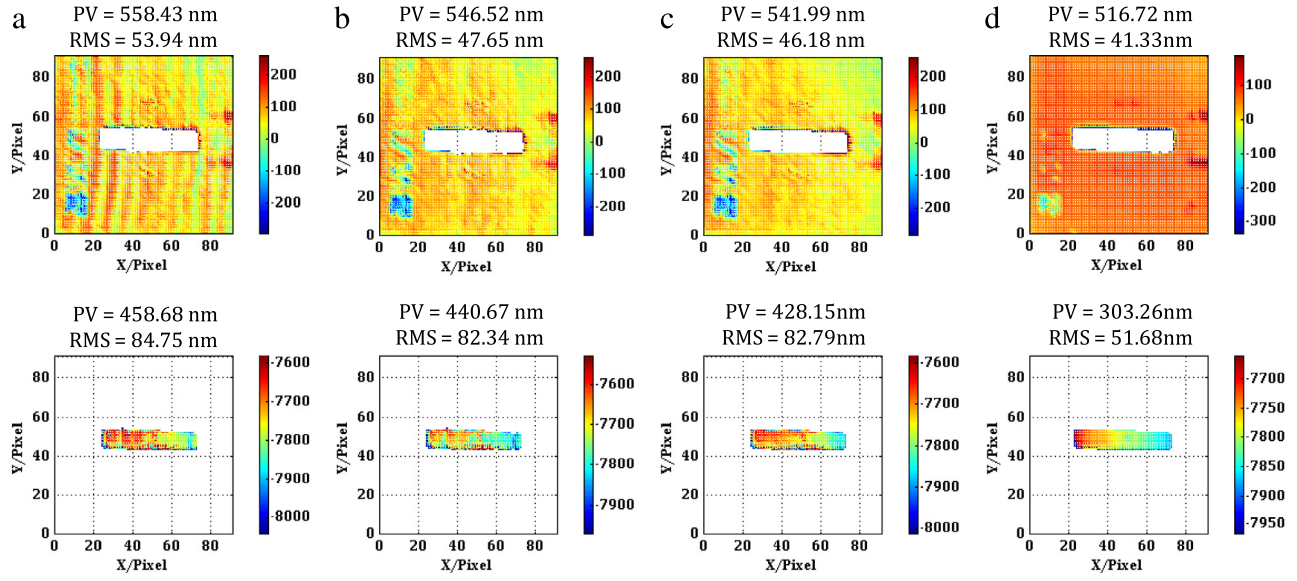

Fig. 8. The distributions of the top and bottom surfaces for the test step demodulated by the four algorithms with the well calibrated phase shifter: (a) 7-frame phase-shift algorithm, (b) $\pi/4$ phase averaging algorithm, (c) the iterative algorithm, (d) the proposed IDS method.

proposed IDS method from the retrieved phase shown in Fig. 9(c) and (d).

Besides, the distributions of the top and bottom surfaces for the test step demodulated by the above four algorithms are also obtained and illustrated in Fig. 11. Caused by the multi-beam interference and the phase-shift error simultaneously for the two wavelengths respectively, the ripple errors are obvious in the forms of moiré fringe in the distributions of the top and bottom surfaces for the 7-frame algorithm and the $\pi/4$ phase averaging algorithm. And the results for IDS method are approximately in agreement with the ones for the iterative algorithm in Fig. 11(c), which also validates the effectiveness of the IDS method in the presences of multi-beam interference as well as the phase-shift error. However, compared with the IDS method, the iterative algorithm needs more multi-beam interferograms and more time for several iterations, which are 24 frames and 5 iterations separately in the experiment. In addition, the results for IDS method are also approximately in agreement with the ones in Fig. 8(d) also by the IDS algorithm in the first experiment.

Above all, we have compared the performances of the four algorithms in the experiment and present the result in Table 1. Obviously, it can be seen from Table 1 that IDS method and Iterative algorithm could suppress the influence of multi-beam interferometry without the calibration of the phase shift. However, the later needs more multi-beam interferograms for the two single wavelengths and iterations to

Table 1
Comparison of the performance for the four algorithms in the experiment.

Approaches		7-frame algorithm	$\pi/4$ phase averaging algorithm	Iterative algorithm	IDS method
Multi-beam interference suppression		No	Yes	Yes	Yes
Calibration of phase shift		Need	Need	No need	No need
Frames of interferograms	λ_1	7	14	24	8
	λ_2	7	14	24	7
Iterations		No	No	5 times	No
Error magnification effect suppression		No	No	No	Yes

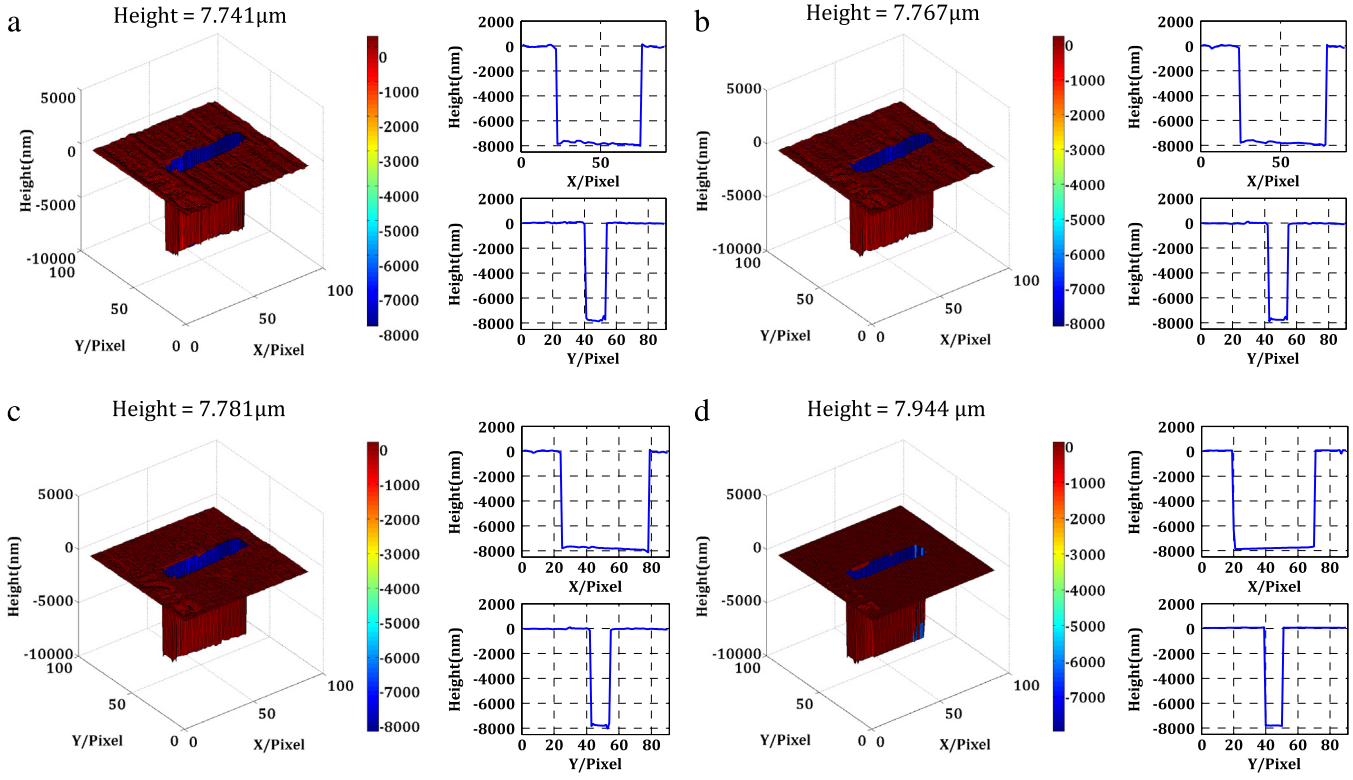

Fig. 9. Experimental results without the calibration of the phase shifter: the demodulated phases of the step 7-frame algorithm in (a), $\pi/4$ phase averaging algorithm in (b), the iterative algorithm in (c), and IDS method in (d).

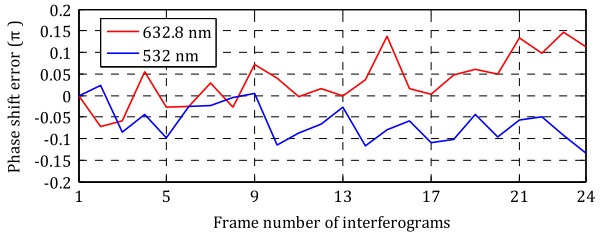

Fig. 10. The phase-shift error of experimental interferograms without the calibration of the phase shifter for the two working wavelengths.

improve the precision. Besides, the error magnification effect in the two-wavelength techniques could not be avoided in the iterative algorithm.

6. Conclusion

In this paper, we analyze the demodulated errors by the conventional phase-shift algorithm such as the de Groot 7-frame algorithm for single wavelength phase in presence of multi-beam interference as well as phase-shift error. The residual phase errors resulted by multi-beam interference and the phase-shift error are less than 0.04 rad and 0.16 rad in practical situation respectively. And to simplify the process of the phase demodulation and to suppress the error magnification effect in dual-wavelength Fizeau interferometer, we propose an integer and decimal portions synthetization (IDS) method. In IDS method, one of the single wavelength wrapped phase is demodulated by the multi-beam interference algorithm, while the second of the single wavelength wrapped phase is extracted by the conventional two-beam interference phase-shift algorithm. And the adopted multi-beam interference algorithm and conventional two-beam interference phase-shift algorithm are our QCSI algorithm and the de Groot's 7-frame phase-shift algorithm separately. From the two single wavelength wrapped phase, the equivalent wavelength unwrapped phase is derived. And then the decimal portion of synthesized phase is obtained directly from the first single wavelength wrapped phase demodulated by QCSI algorithm. Besides, the equivalent wavelength unwrapped phase could determine the fringe order of the first single wavelength wrapped phase to obtain the integer portion of synthesized phase. Combining the integer and decimal portions, we can obtain the final synthesized phase. And the residual phase error of the second single wavelength using the conventional phase-shift algorithm could be suppressed in the calculation for the integer portion of synthesized phase. Compared with other algorithms, the IDS method validates its effectiveness and robustness in simulations and experiment. And IDS method need less frames of the single wavelength

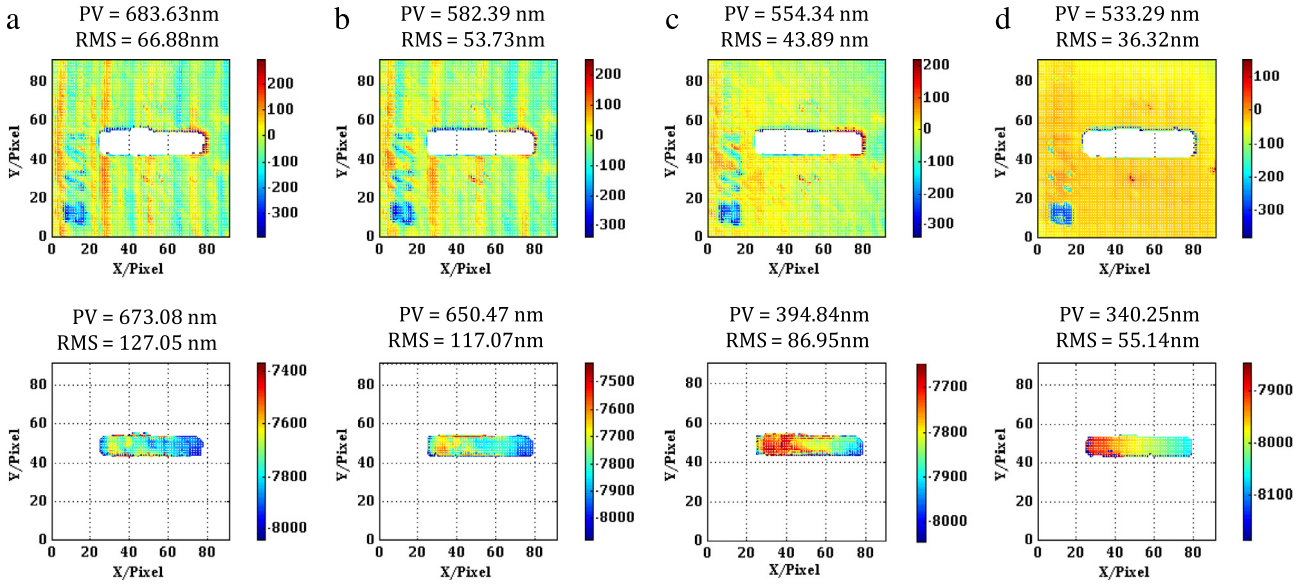

Fig. 11. The distributions of the top and bottom surfaces for the test step demodulated by the four algorithms without the calibration of the phase shifter: (a) 7-frame phase-shift algorithm, (b) $\pi/4$ phase averaging algorithm, (c) the iterative algorithm, (d) the proposed IDS method.

interferograms and no iterations in presence of multi-beam interference as well as phase-shift error.

Acknowledgments

We would like to thank the National Natural Science Foundation of China (61505080, 61377015), the Natural Science Foundation of Jiangsu Province (BK20150788), the Research Fund of the Jiangsu Key Laboratory of Spectral Imaging & Intelligent Sense (3091601410402) and the Opening Project of Key Laboratory of Astronomical Optics & Technology (CAS-KLAOT-KF201604) or financial support.

References

[1] Z. Malacara, M. Servin, Interferogram Analysis for Optical Testing, CRC Press, 2005.
[2] Y.-Y. Cheng, J.C. Wyant, Two-wavelength phase shifting interferometry, Appl. Opt. 23 (1984) 4539–4543.
[3] Y.-Y. Cheng, J.C. Wyant, Multiple-wavelength phase-shifting interferometry, Appl. Opt. 24 (1985) 804–807.
[4] W. Zhang, X. Lu, L. Fei, H. Zhao, H. Wang, L. Zhong, Simultaneous phase-shifting dual-wavelength interferometry based on two-step demodulation algorithm, Opt. Lett. 39 (2014) 5375–5378.
[5] L. Fei, X. Lu, H. Wang, W. Zhang, J. Tian, L. Zhong, Single-wavelength phase retrieval method from simultaneous multi-wavelength in-line phase-shifting interferograms, Opt. Express 22 (2014) 30910–30923.
[6] X. Xu, Y. Wang, Y. Xu, W. Jin, Dual-wavelength in-line phase-shifting interferometry based on two dc-term-suppressed intensities with a special phase shift for quantitative phase extraction, Opt. Lett. 41 (2016) 2430–2433.
[7] P.J. de Groot, Correlated errors in phase-shifting laser Fizeau interferometry, Appl. Opt. 53 (2014) 4334–4342.
[8] W.A. Ramadan, Intensity distribution of Fizeau fringes in transmission with the real path of the interfered multiple-beams, Opt. Lasers Eng. 58 (2014) 27–32.
[9] Q. Yuan, Z. Gao, B. Zhu, X. Cheng, C. Zhang, J. Cheng, An infrared interferometer with a broadband wavelength channel, Opt. Lasers Eng. 51 (2013) 1283–1290.
[10] J. Xu, L. Sun, Y. Li, Y. Li, Principal component analysis of multiple-beam Fizeau interferograms with random phase shifts, Opt. Express 19 (2011) 14464–14472.
[11] J. Vargas, J.A. Quiroga, T. Belenguer, Phase-shifting interferometry based on principal component analysis, Opt. Lett. 36 (2011) 1326–1328.
[12] J. Vargas, J.A. Quiroga, T. Belenguer, Analysis of the principal component algorithm in phase-shifting interferometry, Opt. Lett. 36 (2011) 2215–2217.
[13] Y. Kim, K. Hibino, R. Hanayama, N. Sugita, M. Mitsuishi, Multiple-surface interferometry of highly reflective wafer by wavelength tuning, Opt. Express 22 (2014) 21145–21156.
[14] Y. Kim, K. Hibino, N. Sugita, M. Mitsuishi, Surface profile measurement of a highly reflective silicon wafer by phase-shifting interferometry, Appl. Opt. 54 (2015) 4207–4213.
[15] J. Xu, Q. Xu, L. Chai, H. Peng, Algorithm for multiple-beam Fizeau interferograms with arbitrary phase shifts, Opt. Express 16 (2008) 18922–18932.
[16] T. Hoang, Z. Wang, M. Vo, J. Ma, L. Luu, B. Pan, Phase extraction from optical interferograms in presence of intensity nonlinearity and arbitrary phase shifts, Appl. Phys. Lett. 99 (2011) 031104.
[17] J. Cheng, Z. Gao, Q. Yuan, K. Wang, L. Xu, Carrier squeezing interferometry with $\pi/4$ phase shift: phase extraction in the presence of multi-beam interference, Appl. Opt. 55 (2016) 1920–1928.
[18] M. Servin, M. Cywiak, D. Malacara-Hernandez, J.C. Estrada, J. Quiroga, Spatial carrier interferometry from M temporal phase shifted interferograms: Squeezing Interferometry, Opt. Express 16 (2008) 9276–9283.
[19] B. Li, L. Chen, W. Tuya, S. Ma, R. Zhu, Carrier squeezing interferometry: suppressing phase errors from the inaccurate phase shift, Opt. Lett. 36 (2011) 996–998.
[20] B. Li, L. Chen, C. Xu, J. Li, The simultaneous suppression of phase shift error and harmonics in the phase shifting interferometry using carrier squeezing interferometry, Opt. Commun. 296 (2013) 17–24.
[21] P. de Groot, Derivation of algorithms for phase-shifting interferometry using the concept of a data-sampling window, Appl. Opt. 34 (1995) 4723–4730.
[22] B. Dorrio, J. Blanco-García, C. López, A. Doval, R. Soto, J. Fernández, M. Pérez-Amor, Phase error calculation in a Fizeau interferometer by Fourier expansion of the intensity profile, Appl. Opt. 35 (1996) 61–64.
[23] K. Hibino, B.F. Oreb, D.I. Farrant, K.G. Larkin, Phase-shifting algorithms for nonlinear and spatially nonuniform phase shifts, J. Opt. Soc. Am. A 14 (1997) 918–930.
[24] K. Creath, Step height measurement using two-wavelength phase-shifting interferometry, Appl. Opt. 26 (1987) 2810–2816.
[25] G. Bönsch, H. Böhme, Phase-determination of Fizeau interferences by phase-shifting interferometry, Optik 82 (1989) 161–164.